ELSEVIER

Materials Science and Engineering A265 (1999) 29–41

MATERIALS SCIENCE & ENGINEERING A

Effect of microstructure on wear behavior of Al–Mg–Si alloy matrix–10 vol.% Al_2O_3 composite

S.I. Hong [a,*], Y.S. Seo [b]

[a] *Department of Metallurgical Engineering, Chungnam National University, Taedok Science Town, Taejon, South Korea*
[b] *Metals Research and Development Center, Kia Steel Co., Ltd., Kunsan, South Korea*

Received 4 June 1998; received in revised form 21 December 1998

Abstract

The wear resistance of under-aged and peak-aged 6061 Al–Al_2O_3 particulate composite has been investigated. Peak-aged composites were more wear-resistant than the under-aged composite, while the plane perpendicular to the extrusion direction was more wear-resistant than that parallel to the extrusion direction. The difference of the wear resistance between two different orientations was observed to be greater than that between under-aged and peak-aged matrix microstructures. It shows that preferential orientation of patriculates has a greater effect on the wear resistance than the change of the matrix microstructure. The difference of wear properties between two different orientations was explained by the effect of preferentially orientated reinforcing particles on the shear modulus and shear deformation. The shearing force on the plane perpendicular to the extrusion direction forces the volume beneath a rotating wheel to undergo semi-iso-shear-strain deformation, which requires greater force. The greater resistance to shearing force of the plane perpendicular to the extrusion direction would delay the plastic flow and subsurface damage, which improves the wear resistance.

Keywords: Aging; Mechanically mixed layer; Microstructure; Preferential orientation; Shear force; Sliding speed; Subsurface; Wear

1. Introduction

Metal matrix composites offer considerable potential for enhanced mechanical properties and wear resistance. Interest in discontinuously reinforced metal matrix composites has increased dramatically, partly because they have the advantage of being formable using conventional processing and metal working practices [1–12]. Aluminium alloy matrix composites are currently being considered for a number of engineering applications requiring improved strength, modulus and wear resistance [13–20]. A number of composites exhibit improved wear resistance due to the incorporation of hard constituent into a relatively soft matrix [13–21]. Under some conditions, however, ceramic reinforcement was found to have a negligible effect on the wear resistance [17]. The effect of ceramic reinforcement on the wear properties of aluminium matrix composites is not yet fully understood, partly due to the inherent complexity of many wear process, but the problem is compounded by a possible interplay with microstructural variables in metal matrix composites, such as volume percentage, size, bond strength of the Al matrix and ceramic reinforcement [13–25].

Most of the studies on the wear of metal matrix composites have concentrated on the influences of the type, volume fraction, size and geometry of reinforced ceramics [18,25]. In the case of abrasive wear, the ratio of the diameter of the reinforcement and the size of the abrading particles was found to be of considerable importance [19,22–25]. The mean force transmitted by a single abrading particle is known to increase with the size of abrading particles, which promotes the fracture of reinforced ceramics [26]. This is consistent with the observations by Wang and Hutchings [22] and Wang and Rack [19] that the wear resistance decreased with increasing size of abrading particles. For composites with the same volume fraction, size, distribution and shape of ceramics, high interfacial bond strength and high matrix strength may improve the wear perfor-

* Corresponding author. Tel.: +82-42-8216595; fax: +82-42-8229401.
E-mail address: sihong@hanbat.chungnam.ac.kr (S.I. Hong)

0921-5093/99/$ - see front matter
PII: S0921-5093(99)00006-4

mance [13,14,27–31]. Wang and Rack [27] and Lin and Liu [31] reported that wear resistance can be improved by proper heat treatment of 2XXX and 7XXX Al alloy matrix composites, suggesting the matrix microstructure and, possibly interfacial strength [32,33], play important roles in wear of Al alloy matrix composites.

Since most variables which affect the wear behaviors of composites are interdependent [25], it is difficult to draw a clear conclusion even from the results of well-designed and prepared wear experiments [34]. Understanding of wear characteristics of composites is far from complete and more data and results on wear of composites should be collected in statistical manner for effective correlations to be made. The purpose of the present study is to investigate the wear properties and damage in an Al–Mg–Si alloy matrix composite reinforced with 10 vol.% Al_2O_3 as a function of wear parameters, such as sliding speed and applied load. For better understanding of the effect of microstructural variables on the wear behaviors of Al alloy matrix composites, the correlation between the wear properties and the microstructural evolution in an Al–Mg–Si alloy matrix composite reinforced with 10 vol.% Al_2O_3 was examined.

2. Experimental

The Al–Mg–Si alloy (6061 Al) matrix composite reinforced with 10 vol.% α-Al_2O_3 (nominal size, 13 μm) selected for this study was produced by a molten metal method and extruded into a rod with a diameter of 25 mm, the extrusion ratio being 12:1. The as-received composite was solution treated at 550°C for 2 h and water quenched to room temperature, naturally aged at room temperature for 24 h. and artificially aged. The under-aged condition was obtained by heat treating at 178°C for 30 min. The peak-aged condition was obtained by heat treating at 178°C for 8 h. Some samples were cut parallel to the extrusion direction before testing for transmission electron microscopy (TEM) characterization; detailed sample preparation method is given elsewhere [35]. To evaluate the effect of the aging and the preferred particle orientation on the hardness, Rockwell hardness measurements on a B scale were made. Wear properties were examined utilizing a disk and block-type Ohgoshi wear tester. The configuration of the Ohgoshi-type wear tester is schematically shown in Fig. 1 [36].

A high carbon chromium steel (0.61% C, 0.82% Mn, 0.15% Si and 0.80% Cr) disk (Rockwell hardness, HRc = 43) was driven by a motor at variable speeds, and the sliding distance was calculated by multiplying the rotation speed by the circumference of the disk. The radius and the thickness of the disk were 15 and 3 mm, respectively. Both the disk and composite samples were ground against 400 grit SiC paper and then cleaned in methanol before testing. The arithmetic average surface roughness R_a of the disk after grinding was 1.6 μm and that of composite samples was 1.8 μm. The sliding speed was varied from 0.51 to 3.62 m/s and the contact load was varied from 21 to 123 N. For all tests in this study, the total sliding distance travel was fixed at 100 m. In order to measure the steady-state temperature, a hole, 2 mm in diameter, was machined through the thickness in the center of the expected sliding track and a K-type thermocouple was inserted from the bottom and attached to the inner surface of the hole approximately 2 mm below the final wear surface, which was predicted based on the experimental data in this study. After testing, the wear surfaces were examined using scanning electron microscopy (SEM). Some of the worn samples were sectioned perpendicular to the sliding direction using a low-speed diamond saw and examined using SEM.

3. Experimental results

3.1. Microstructure and mechanical properties

SEM micrographs of two planes parallel and perpendicular to the extrusion direction are shown in Fig. 2a and Fig. 2b, respectively. A close look at the shape of particles on the plane parallel to the extrusion direction (Fig. 2a) reveals anisotropy in the particle alignment in the extrusion direction (indicated by an arrow) as compared to the other directions, although the shape of Al_2O_3 particles was observed to be irregular on the plane perpendicular to the extrusion direction(Fig. 2b). The preferred orientation distribution of the particulates, evidently the result of the extrusion process [37], may have an effect on the anisotropic properties of composites.

Quantitative information on the aspect ratio distribution and orientation distribution of particles was obtained from the image analysis. Fig. 3a,b shows the aspect ratio distribution on the planes parallel (Fig. 3a) and perpendicular (Fig. 3b) to the extrusion direction.

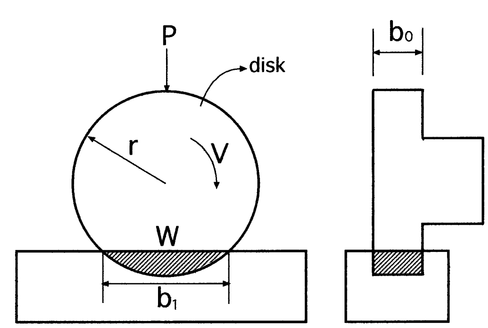

Fig. 1. Schematic configuration of Ohgoshi wear tester.

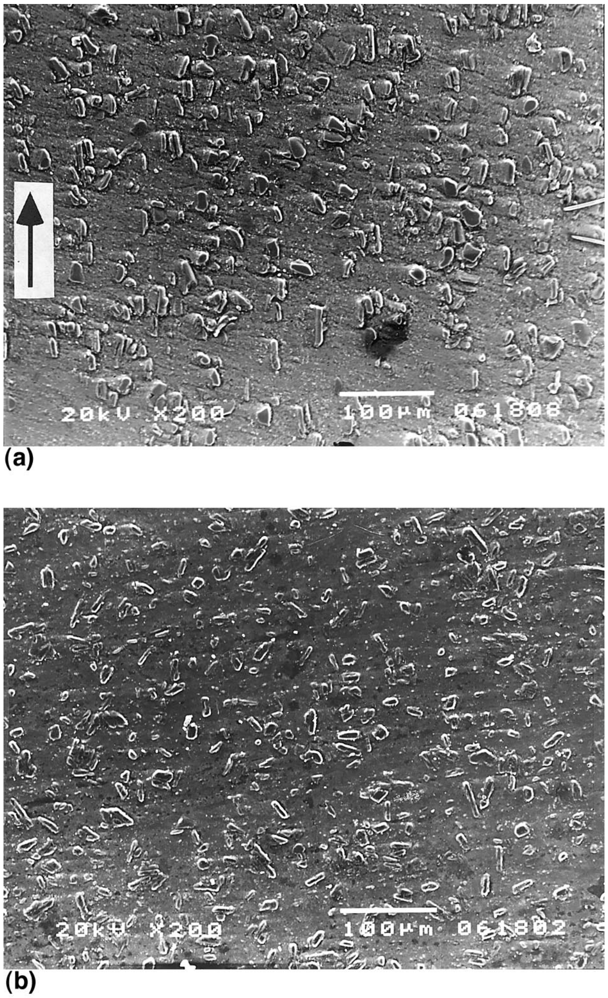

Fig. 2. SEM micrographs of the planes parallel (a) and perpendicular (b) to the extrusion direction.

The average aspect ratio on the plane perpendicular to the extrusion direction was found to be 3.9, which is greater than that (3.1) on the plane parallel to the extrusion direction. The orientation distributions on the planes parallel (Fig. 4a) and perpendicular (Fig. 4b) to the extrusion direction show more clear difference between these two planes. The orientation angle was measured with respect to the line perpendicular to the extrusion direction on the plane parallel to the extrusion direction, whereas the orientation angle on the plane perpendicular to the extrusion direction was measured with respect to an arbitrary line drawn on the plane since the microstructural variables are supposed to be symmetrical with respect to the extrusion axis. As shown in Fig. 4, the orientation distribution on the plane parallel to the extrusion direction (Fig. 4a) shows a pronounced preference for the particles to lie along the extrusion direction (90°). On the other hand, the orientation distribution on the plane perpendicular to the extrusion direction (Fig. 4b) shows random distribution of particles.

Fig. 5a and Fig. 5b show the matrix microstructure of the under-aged and peak-aged composites, respectively. The under-aged composite was found to contain very small G.-P. zones throughout the Al matrix. Fig. 5a shows the dark field micrograph of the under-aged matrix in which the very small spherical white spots are the G.-P. zones. In the peak-aged composite (Fig. 5b), Mg_2Si needles [38–41] were observed throughout the matrix.

In Table 1, the Rockwell hardnesses (B scale) of the under-aged and the peak-aged composites on the planes parallel and perpendicular to the extrusion direction are summarized. The values reported in Table 1 were averaged from at least ten readings. In case of Rockwell hardness, the indentation covers a large volume containing a large number of particles and each measurement may represent the relatively accurate average of bulk properties including ceramic particles. The peak-aged composite was found to be harder than the under-aged composite. Since the scatter of the Rockwell hardness data is relatively small, the small difference of the hardness between two different orientations may have a physical validity. The plane perpendicular to the extrusion direction was observed to be slightly harder in the under-aged composite, but the difference does not appear to be large enough to influence the wear resistance in the peak-aged composite. The small difference of the Rockwell hardness between two different orientations may be associated with the orientation dependence of the elastic modulus of ceramic particles [37].

3.2. Wear properties

In this study, the specific wear rate, which is the volume of wear loss per unit load and unit sliding distance [36], was used to express the wear rate. The specific wear can be determined by using the following approximation.

$$W = b_1^3 b_o / 8rPd \tag{1}$$

where P is the final load; r is the radius of the disk; b_o is the thickness of disk; b_1 is the length of the sliding track, and d is the sliding distance (see also Fig. 1).

Fig. 6 shows the variation of the specific wear of planes parallel and perpendicular to the extrusion direction in the under-aged and peak-aged composites as a function of sliding speed. The specific wear rate was found to increase with increase of sliding speed probably due to friction heating. As shown in this figure, the plane perpendicular to the extrusion was more wear-resistant than the plane parallel to the extrusion direction. Additionally, the peak-aged composite was more wear-resistant than the under-aged composites. In Fig. 7, the specimen temperature is plotted against the sliding speed at the applied load of 62 N for the peak-aged composite of the present study. The difference of the specimen temperature between the under-aged and the peak-aged composites was found to be negligible. The specimen temperature was observed to increase continuously with increasing sliding speed, reaching120°C at 4 m/s. In Fig. 8, the specific wear rate of planes parallel and perpendicular to the extrusion direction in the under-aged and peak-aged composites is plotted as a function of final load. The specific wear rate was found to increase with increase of load as expected. The figure also shows that the plane perpendicular to the extrusion direction was more wear-resistant than that parallel to the extrusion direction and that the peak-aged composites was more wear-resistant than the under-aged composites over the whole load range of this study.

The worn surfaces of the composites were observed using SEM to examine the mode of wear loss. SEM micrographs of the worn surfaces of the under-aged

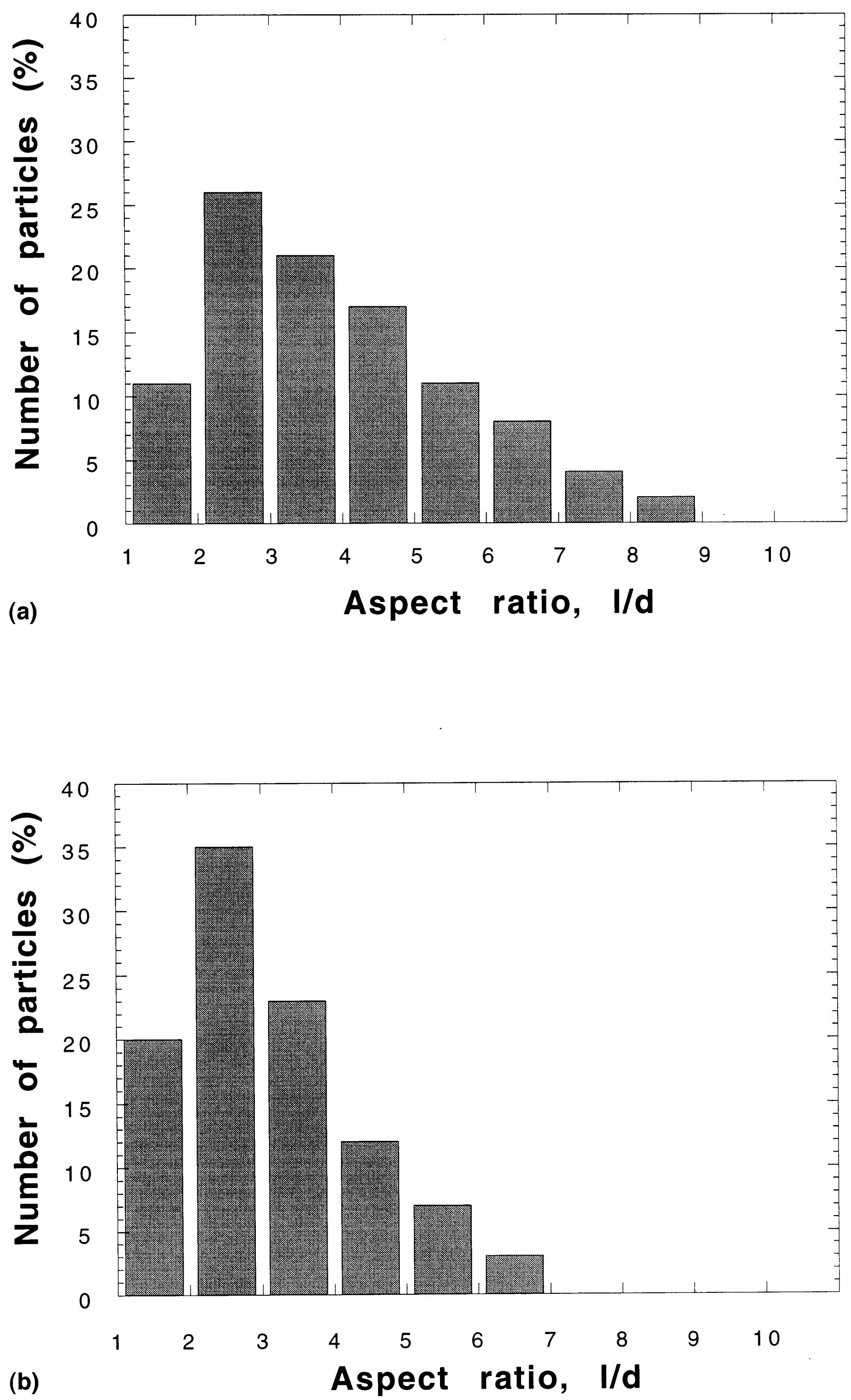

Fig. 3. Aspect ratio distribution of Al_2O_3 particulates on the planes parallel (a) and perpendicular (b) to the extrusion direction.

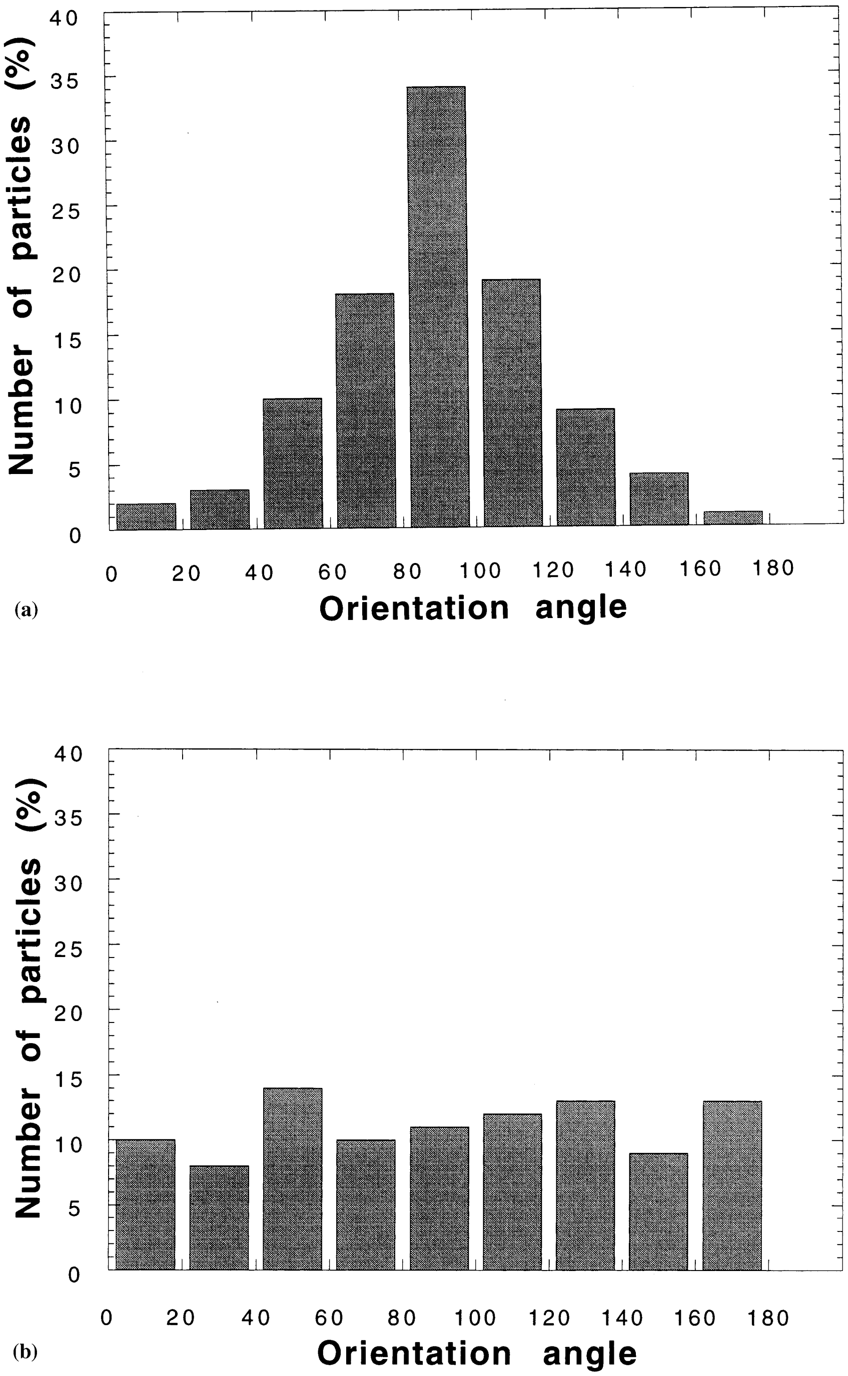

Fig. 4. Orientation distribution of Al_2O_3 particulates on the planes parallel (a) and perpendicular (b) to the extrusion direction. The orientation angle was measured with respect to the line perpendicular to the extrusion direction on the plane parallel to the extrusion direction (a), whereas the orientation angle on the plane perpendicular to the extrusion direction (b) was measured with respect to an arbitrary line drawn on the plane.

and peak-aged composites which are parallel to the extrusion direction are shown as a function of sliding speed in Fig. 9. The depth of subsurface affected by the shear force of the rotating wheel increased drastically with increase of sliding speed as clearly shown in Fig. 9. As shown in this figure, no pronounced difference in wear surface morphologies due to different heat treatments were detected by SEM. The presence of grooves and wear sheets was observed to be more evident with increase of sliding speed, indicating the shear plastic flow increased with increase of sliding speed. The general feature of the worn surfaces of the under-aged and peak-aged composites which are perpendicular to the extrusion direction appeared to be quite similar to those shown in Fig. 9.

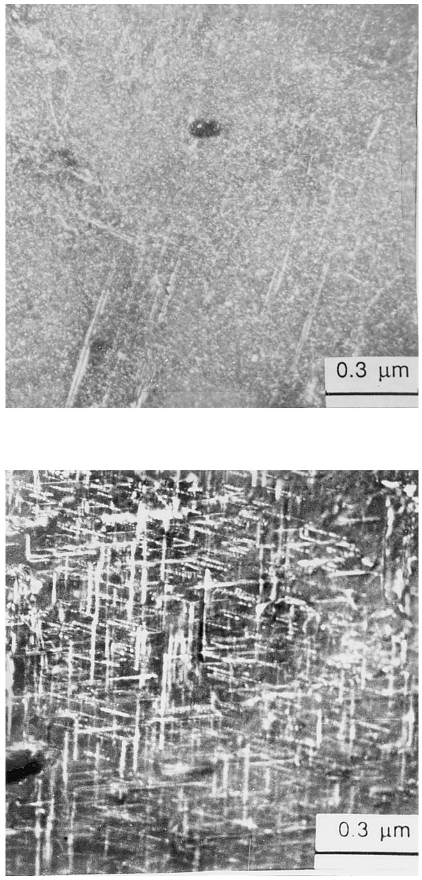

Fig. 5. (a) Dark field TEM micrograph showing small spherical zones in the under-aged composite: (b) Dark field TEM micrograph showing Mg2Si needles in the peak-aged composite. Both micrographs were taken using a {111} reflection in a ⟨110⟩ zone.

Fig. 10 shows the profile of the sectioned under-aged and peak-aged composites in which the worn surface is perpendicular to the extrusion direction. The plane of the micrographs is perpendicular to the sliding direction and the worn surface is towards the top of the micrographs. The extrusion direction of the composites is vertical in Fig. 10. As shown in these micrographs, the presence of the surface layer with fine particles by fragmentation was most evident when the sliding speed was 1.14 m/s. The surface layer with fine particles are indicated by brackets in Fig. 10b,e. When the sliding speed was lower (0.51 m/s) and higher (3.61 m/s), the size of Al_2O_3 particles in the near-surface region was not found to be different from that far away from the surface. The profile of the sectioned under-aged and peak-aged composites in which the worn surface is parallel to the extrusion direction showed similar morphologies as shown in Fig. 10, and the surface layer with fine particles was most evident when the sliding speed was 1.14 m/s.

Table 1
Rockwell hardness (B scale) of the composites studied

	Perpendicular		Parallel	
	Under-aged	Peak-aged	Under-aged	Peak-aged
Rockwell hardness (HR_B)	44.5 ± 2.1	64.6 ± 0.9	41.3 ± 1.4	63.1 ± 1.0

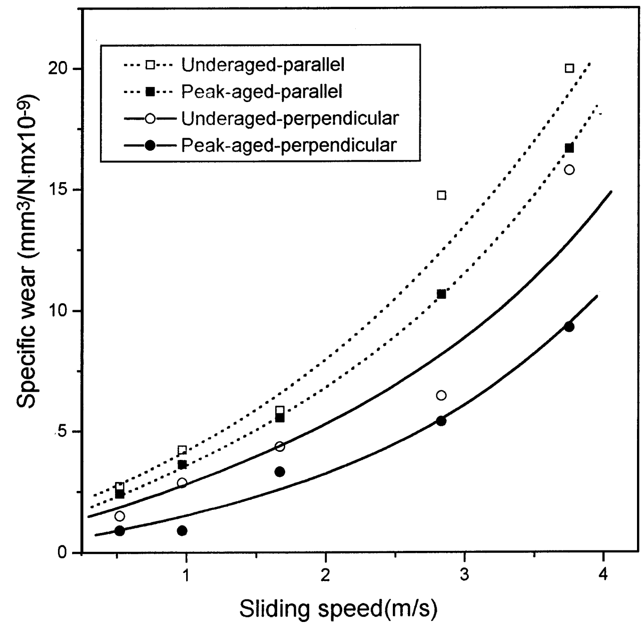

Fig. 6. The variation of the specific wear of planes parallel and perpendicular to the extrusion direction in the under-aged and peak-aged composites as a function of sliding speed.

4. Discussion

As shown in Fig. 6, the specific wear increased by a factor of 5–10 with the increase of sliding speed from 0.51 to 3.62 m/s at the same applied load. The increase of the sliding speed is thought to increase the shear deformation rate of the near-surface layer and the temperature due to friction heating. Indeed, the specimen temperature near the surface (2 mm below the wear surface), due to friction heating, reached 120°C at the highest sliding speed employed in this study. The real temperature on the surface is believed to be higher than 120°C since the temperature increases quite rapidly near the surface [34]. The ratio of the applied load to the matrix strength would increase with increasing sliding speed, even at constant applied load since the matrix strength decreases due to friction heating at high sliding speeds. Therefore, the increase of the sliding speed may have the similar effect to the increase of the applied load, since the matrix strength decreases with the increase of sliding speed because of the friction heating.

It is now generally accepted that plastic deformation in the near-surface region is prevalent in wear process

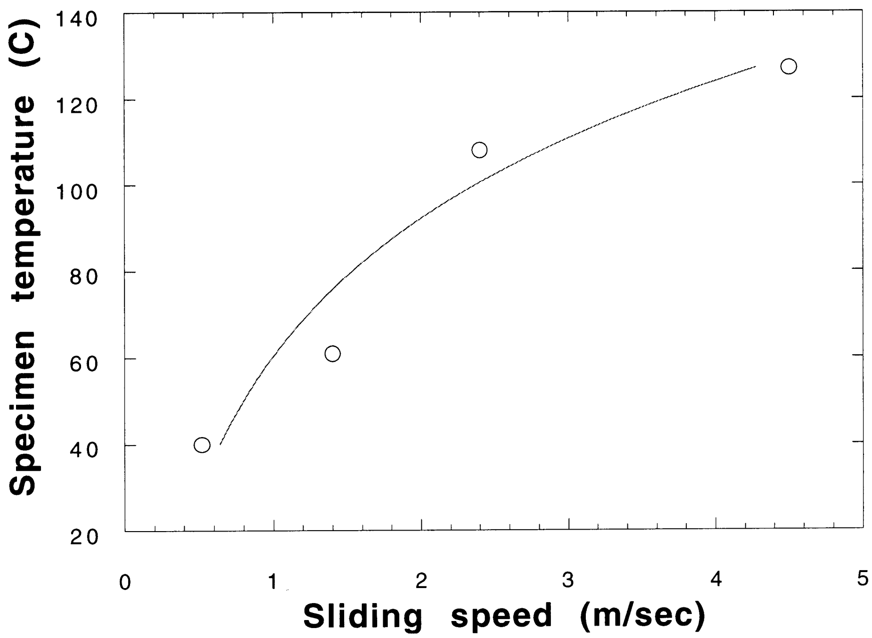

Fig. 7. Steady-state temperature versus sliding velocity at the applied load of 62 N for the peak-aged composites.

of most materials [42–45]. Rigney and his co-workers [42–44] examined the sub-surface region of worn materials and observed cellular microstructure or dislocation tangles, which present a suitable pathway for separation of wear debris from the surface. They [42–44] suggested that the plastic deformation changes the near-surface microstructure in ways which make the material unstable to local shear. The deformation morphology observed in the near-surface region on Al metal matrix composites [13,14] suggests that similar substructures may develop in Al metal matrix composites after wear testing.

In Fig. 11, the effect of the sliding speed on the depth of the plastic flow is illustrated schematically. In this figure, it can be assumed that the effect of the sliding speed on the shearing stress due to a rotating disk is negligible, and the maximum temperature due to friction heating increases with sliding speed. The shearing stress caused by the rotating disk would decrease gradually with increasing depth from the wear surface as illustrated in Fig. 11. Since the temperature due to friction heating would also decrease with increasing depth until it reaches the equilibrium temperature, the flow stress of the matrix would increase gradually with increasing depth until it attains the flow stress at the equilibrium temperature.

In Fig. 11, the region where the shearing stress exceeds the flow stress would experience plastic flow and the depth of plastic flow can thus be determined. As shown in Fig. 11, the flow stress level in the near-surface region would decrease with sliding speed since the temperature due to friction heating increases with sliding speed, and the depth of plastic flow, therefore, would increase with sliding speed. The worn surface (Fig. 9) clearly indicates that the shear plastic flow increased with increase of sliding speed. The increase of the specific wear rate with increasing sliding speed is thought to be associated with the increase of the friction heating. The depth of the plastic zone is also expected to increase rapidly with increasing load, since the increase of the shearing stress and the friction heating also increase with increasing load (Fig. 8).

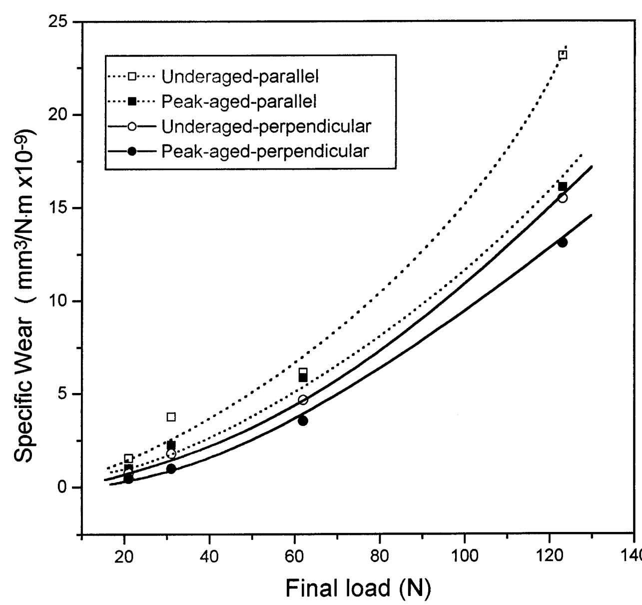

Fig. 8. The specific wear of planes parallel and perpendicular to the extrusion direction in the under-aged and peak-aged composites as a function of final load.

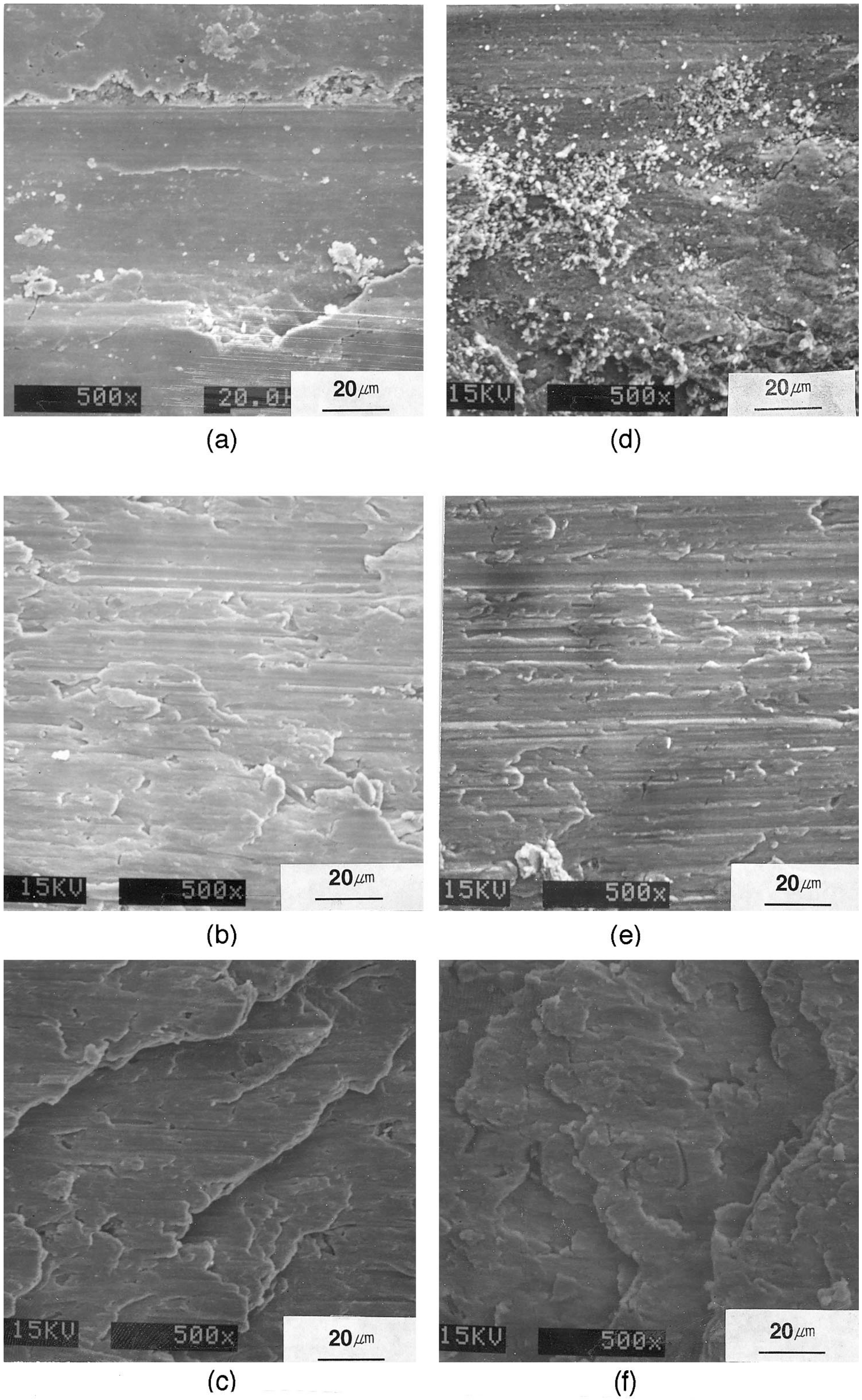

Fig. 9. SEM micrographs of the worn surfaces of the under-aged (a–c) and peak-aged (d–f) composites which are parallel to the extrusion direction are shown as a function of sliding speed. The final load was 62 N. (a,d) Sliding speed, 0.51 m/s; (b,e) sliding speed, 1.14 m/s; (c,f) sliding speed, 3.62 m/s.

The depth of the surface affected by sliding wear appear quite shallow at a sliding speed of 0.51 m/s and the test load of 62 N as shown in Fig. 10. When the sliding speed is very low, the depth of the subsurface affected by the shear force is very shallow, and the oxidation rate may be faster than the wear and removal

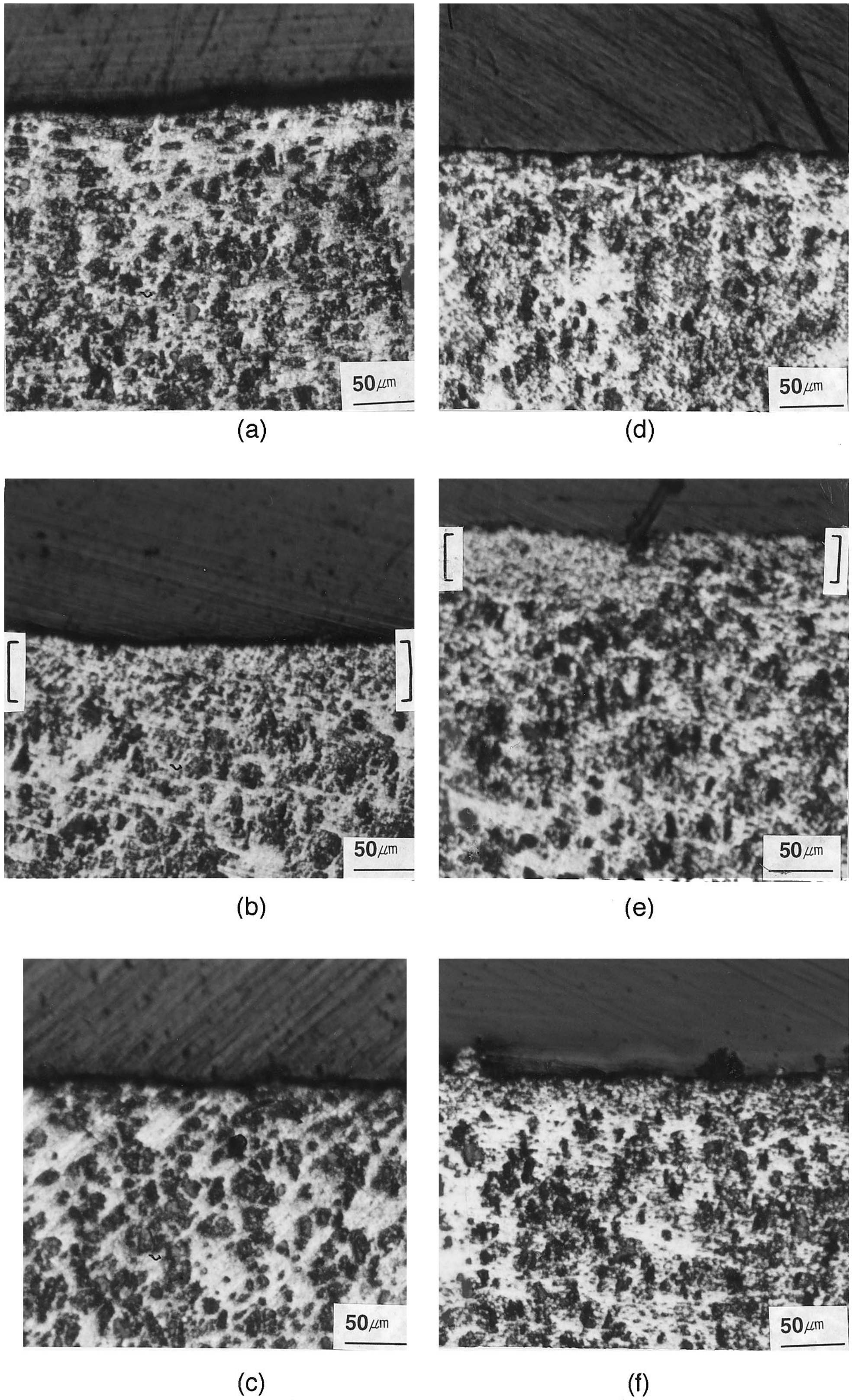

Fig. 10. The profile of the sectioned under-aged (a–c) and peak-aged (d–f) composites in which the worn surface is perpendicular to the extrusion direction. The final load was 62 N. (a,d) Sliding speed, 0.51 m/s; (b,e) sliding speed, 1.14 m/s; (c,f) sliding speed, 3.62 m/s.

rate of surface [46]. In this case, the wear rate may decrease with the formation of the surface oxide layer. Since the depth of the surface layer is shallower compared to the size of particles [13,14], and the resistance of the matrix to the plastic flow is high due to relatively low friction heating and the presence of the surface oxide layer, the incidence of Al_2O_3 particle fracture and mechanical milling may be negligible.

One interesting observation in this study is that the wear properties are dependent on the orientation. Although the compressive strength and hardening behavior were found to be greatly influenced by the matrix microstructure, the effect of the matrix microstructure on the wear properties is not as pronounced as that of the orientation. The relatively weak dependence of wear resistance on the matrix microstructure (under-aged versus peak-aged) may be explained by the stress–strain responses of the under-aged and the peak-aged composites [47]. The difference of flow stresses between the under-aged and the peak-aged composites narrowed with increasing strain. The plastic flow near the surface region during wear is very severe and the difference of strength caused by the difference of the matrix microstructure may be small, resulting in the relatively weak dependence of wear resistance on the matrix microstructure. Vaidya and Zurek (unpublished) found that the difference of the flow stresses of 8090 Al matrix composite at the true strain of 0.1 between the extrusion direction (300 MPa) and the direction perpendicular to the extrusion (280 MPa) was 20 MPa. The difference of the flow stresses between the extrusion direction and the direction perpendicular to the extrusion was also found to be negligible in 6061 Al matrix composite [47]. Therefore, the orientation difference of wear resistance cannot be explained by the difference of the flow stresses between planes parallel and perpendicular to the extrusion direction (Vaidya and Zurek, unpublished work).

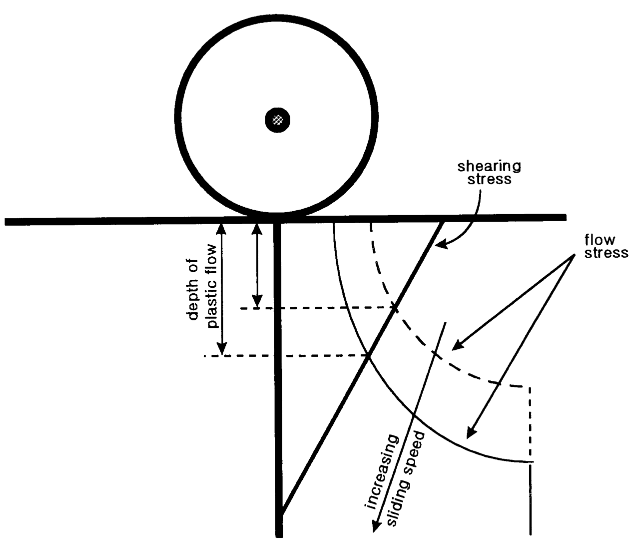

Fig. 11. A schematic representation illustrating the way the depth of plastic flow can be determined.

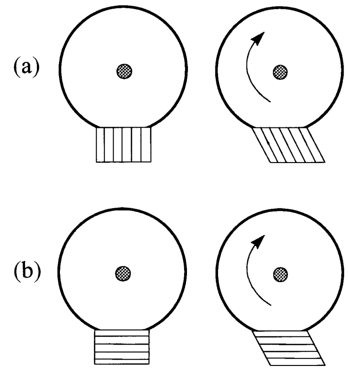

Fig. 12. A rotating wheel on a part of the composite block. (a) The shearing force on the plane perpendicular to the extrusion direction the volume beneath a wheel to undergo iso-shear-strain deformation. (b) The shearing force on the plane parallel to the extrusion direction forces the volume beneath a wheel to undergo iso-shear-stress deformation.

The difference of wear properties between two different directions may be explained by the effect of the preferentially oriented reinforcing particles on the shear modulus and shear deformation as schematically presented in Fig. 12. In this figure, the square represents the part of composites which is under the influence of the shear force caused by a rotating wheel, and the lines in the square represent the preferential orientation of the reinforcing particles. It may be assumed that the preferentially oriented particles behave as continuous fibers in the small area, as shown in Fig. 12, to simplify the discussion. In discontinuously reinforced composites, as in this study, the effect of the preferential orientation on the shear deformation is not as effective as that described in Ref. Fig. 12. Nevertheless, the shear deformation near the wear surface will be influenced by preferentially oriented particles. The shearing force on the plane perpendicular to the extrusion direction, as shown in Fig. 12a, caused by a rotating wheel, forces the volume beneath a wheel to undergo iso-shear-strain deformation. On the other hand, the shearing force on the plane parallel to the extrusion direction, as shown in Fig. 12b, forces the volume beneath a wheel to undergo iso-shear-stress deformation. It is well known that the composite modulus for isostrain deformation is greater than that for isostress deformation [48]. Indeed, Jeong et al. [37] observed that the in-plane shear modulus was 7–10% higher than those of other directions. Therefore the resistance to shearing force would be greater on the plane perpendicular to the extrusion direction, which is consistent with the observation in Fig. 6and Fig. 8. Rigney and Glaeser [42] suggested that anything which delays the plastic flow and the formation of the cellular structure will delay the stage of wear. If the reinforced particles are rigid enough, preferentially oriented particles perpendicular to the wear surface, as in Fig. 12a, would delay the plastic flow and the wear rate. The small difference of the hardness between two different orientations (Table 1) may have contributed to the difference of the wear resistance.

Since wear is a very complex problem and, in most cases, the removal of material during wear occurs by fracture and fatigue processes [45,49–51], the effect of preferentially oriented ceramics given in Fig. 12 may not be valid if the particles or whiskers crack more or less easily under the influence of shearing force. If the fracture of preferentially orientated particles or whiskers, as in Fig. 12a, occurs easily, they cannot resist the shearing force and, therefore, cannot delay the shear deformation of the near-surface region, which may result in inferior wear resistance. Wang and Rack [17,19] also examined the effect of whisker orientation on wear of SiC-whisker-reinforced 7091 Al matrix composites. Their result shows that, in the case of abrasive wear, the plane perpendicular to the extrusion direction is more wear resistant than that parallel to the extrusion direction, as in this study, if the abrasive particle diameters are smaller than 60 μm [19]. The reverse is the case at abrasive particle diameters greater than 60 μm. Under unlubricated sliding conditions [17], the plane parallel to the extrusion direction was found to be more wear resistant, in contradiction to the observation of the present study. These seemingly contradictory results may be associated with the difference of the size, shape and distribution of ceramic particles or whiskers.

The critical load F^* to cause fracture of a long brittle fiber supported in a ductile matrix may be given by the following equation;

$$F^* = \alpha d^2 (3\pi\sigma_f H_m)^{1/2} \tag{2}$$

where d is the diameter of the fiber, σ_f is its tensile strength, H_m is the hardness of the matrix and α is a parameter dependent on the orientation of the fiber with respect to the stress axis. It should be noted that the fracture load decreases with decreasing fiber diameter. Although the above equation was developed for fiber-reinforced composites, it may be used to predict the general trend of the fracture load F^* for whisker or particulate-reinforced composites with or without minor modification. The effect of the orientation of ceramic reinforcement (with the aspect ratio greater than the unity) on the wear behavior of metal matrix composites may depend on the diameter and the aspect ratio of the ceramics. When the diameter of the reinforced ceramics is relatively large, they may not crack easily and can resist the shear deformation. Therefore, the resistance to shearing force would be greater when the preferentially oriented particlulates, whiskers or fibers are lying perpendicular to the wear surface, as observed in this study (see Fig. 6, Fig. 7and Fig. 12). The average diameter of the ceramic particulates in the 6061 Al matrix composites of the present study was approximately 4 μm, whereas that of the ceramic whiskers in 7091 Al matrix composites studied by Wang and Rack [17,19] was 0.5 μm.

When the diameter of the reinforced ceramics is relatively small, as in the study by Wang and Rack, they may crack easily and the orientation dependence of the shear modulus (Fig. 12) may not play an important role. Rather, the mechanically mixed surface layer of the matrix and ceramic fragments may play an important role. In this case, the mechanically mixed layer formed on the plane with higher area fraction of ceramics will be harder since it would contain more ceramic fragments and the plane with higher area fraction of ceramics (i.e. the plane to which preferentially oriented particles, whiskers or fibers lies parallel) would be more wear resistant, as observed by Wang and Rack [17,19]. The suggestion on the orientation dependence of the wear resistance given above is consistent with the observation of Wang and Rack [19]. They observed that the plane perpendicular to the extrusion direction is more wear-resistant than that parallel to the extrusion direction at abrasive particle diameter below 60 μm in SiC-whisker-reinforced 7091 Al metal matrix composites and the effect was reversed when coarser abrasives were used.

The critical abrasive particle diameters D_c, above which the fiber fracture occurs in abrasive wear of alumina fiber-reinforced 6061 Al matrix composites, were observed to be 20–40 μm [22]. It may be assumed that 60 μm is the critical abrasive diameter for fracture in SiC_w-reinforced 7091 Al matrix composites. In this case, at abrasive particle diameters below 60 μm, reinforced SiC_w may not crack easily and the resistance to shearing force and wear resistance would be greater (see also Fig. 6, Fig. 7 and Fig. 12) when the preferentially whiskers are lying perpendicular to the wear surface, as observed by Wang and Rack [19]. At abrasive particle size larger than 60 μm, ceramics may crack easily and the orientation dependence of the shear modulus (Fig. 12) may not play an important role. In this case, the mechanically mixed layer formed on the plane with higher area fraction of ceramics will be harder, as explained above, and wear resistance would be greater (see also Fig. 6, Fig. 7and Fig. 12) when the preferentially whiskers are lying parallel to the wear surface, as observed by Wang and Rack [19].

The observation that the effect of preferentially oriented particles has a greater effect on the wear properties than the effect of the matrix microstructure in the present study suggests that the wear resistance of composites cannot be directly related to their strength. Recently, Venkataraman and Sundararajan [13,14] also observed that the wear resistance of composites has no linear relationship with their hardness. They [13,14] suggested that the overall wear resistance of the composites is determined not by the relative strengths of the matrix and the particulates but by the relative wear resistance of the matrix and particulates. This explains why the presence of relatively big hard particles has a greater influence on the wear resistance than on the strength.

5. Conclusions

Based upon a study of the mechanical response and microstructural evolution of Al–Mg–Si alloy matrix composites, the following conclusions can be drawn:

(1) The peak-aged composite was more wear resistant than the under-aged composite, and the plane perpendicular to the extrusion direction was more wear resistant than that parallel to the extrusion direction.

(2) The difference of wear properties between two different directions can be explained by the effect of preferentially orientated reinforcing particles on the shear modulus and shear deformation. The shearing force on the plane perpendicular to the extrusion direction is thought to force the volume beneath a rotating wheel to undergo semi-iso-shear-strain deformation, which requires greater force.

(3) The presence of grooves and wear sheets was observed to be more pronounced with increase of sliding speed and applied load, indicating the plastic shear flow increased with increase of sliding speed and applied load.

(4) The subsurface layer with fine Al_2O_3 fragments, which may act as a protective layer, was observed at a sliding speed of 1.14 m/s. When the sliding speed was increased to 3.62 m/s, the presence of the subsurface layer with fine particles was much less pronounced and the specific wear increased drastically.

Acknowledgements

This work was supported by Korea Science and Engineering Foundation under contract 97-0300-0701-3. The authors are grateful to Mr D.H. Kim for measuring the temperature rise during wear testing and to Mr D.Y. Maeng for conducting compression tests. The help of Ms M.J. Chang in analyzing microstructural anisotropy is also gratefully acknowledged.

References

[1] J.M. Papazian, P.N. Adler, Metall. Trans. 21A (1990) 401.
[2] J.J. Lewandowski, C. Liu, W.H. Hunt Jr., Mater. Sci. Eng. 107A (1989) 241.
[3] D.L. Davidson, Metall. Trans. 22A (1991) 113.
[4] R.J. Arsenault, Mater. Sci. Eng. 64 (1984) 171.
[5] Y. Flom, R.J. Arsenault, Acta. Metall. 37 (1989) 2413.
[6] S.I. Hong, G.T. Gray III, Acta Metall. 40 (1992) 3299.
[7] S.V. Kamat, J.P. Hirth, R. Mehrabian, Acta Metall. 37 (1989) 2395.
[8] Y.L. Klipfel, M.Y. He, R.M. McMeeking, A.G. Evans, R. Mehrabian, Acta Metall. Mater. 38 (1990) 1063.
[9] S.I. Hong, G.T. Gray III, K.S. Vecchio, Mater. Sci. Eng. 171A (1993) 181.
[10] S.I. Hong, G.T. Gray III, J.J. Lewandowski, Acta Metall. Mater. 41 (1993) 2337.
[11] S.I. Hong, G.T. Gray III, J. Mater. Sci. 29 (1994) 2987.
[12] S.I. Hong, G.T. Gray III, J.J. Lewandowski, Scripta Metall. Mater. 27 (1992) 431.
[13] B. Venkataraman, G. Sundararajan, Acta Matall. Mater. 44 (1996) 451.
[14] B. Venkataraman, G. Sundararajan, Acta Matall. Mater. 44 (1996) 461.
[15] J.W. Liou, L.H. Chen, T.S. Lui, J. Mater. Sci. 30 (1995) 285.
[16] S. Wilson, A. Ball, in: K. Fredrich (Ed.), Advances in Composite Tribology, Elsevier, Amsterdam, 1993, p. 311.
[17] A. Wang, H.J. Rack, Mater. Sci. Eng. A147 (1991) 211.
[18] T.W. Clyne, P.J. Withers, An Introduction to Metal Matrix Composites, Cambridge University Press, Cambridge, 1993, p. 294.
[19] A. Wang, H.J. Rack, Wear 146 (1991) 337.
[20] Z.F. Zhang, L.C. Zhang, Y.W. Mai, J. Mater. Sci. Eng. 30 (1995) 1961.
[21] N. Axen, S. Jacobson, Wear 174 (1994) 187.
[22] A.G. Wang, I.M. Hutchings, Mater. Sci. Technol. 5 (1989) 71.
[23] J. Singh, A.T. Alpas, Metall. Mater. Trans. 27A (1996) 3135.
[24] A.T. Alpas, J. Zhang, Metall. Mater. Trans. 25A (1994) 969.
[25] A.P. Sannino, H.J. Rack, Wear 189 (1995) 1.
[26] I.M. Hutchings, in: T.W. Clyne and P.J. Withers (Eds.), Proceedings of the 2nd European Conference on Adv. Mater., Euromat 91, Inst. of Metals, Cambridge, UK, 1991, p. 56.
[27] A. Wang, H.J. Rack, in: R.B. Bhagat, A.H. Clauer, P. Kumar, A.M. Ritter (Eds.), Metal and Ceramic Matrix Composites: Processing, Modelling and Mechanical Behavior, TMS, Warrendale, PA, 1990, p. 487.
[28] J.E. Allison, G.S. Cole, J. Metals 45 (1993) 19.
[29] A. Sato, R. Mehrabian, Metall. Trans. 7B (1976) 443.
[30] M.K. Surappa, S.V. Prasad, P.K. Rohatgi, Wear 77 (1982) 295.
[31] S.-J. Lin, K.-S. Liu, Wear 121 (1988) 1.
[32] M. Manoharan, J.J. Lewandowski, Acta Metall. Mater. 38 (1990) 489.
[33] R.S. Haaland, G.M. Michal, G.S. Chottiner, in: M.N. Gungor, P.K. Liaw III (Eds.), Fundamental Relationships Between Microstructures and Mechanical Properties of Metal Matrix Composites, TMS, Warrendale, PA, 1990, p. 779.
[34] S.C. Lim, M.F. Ashby, Acta Metall. 35 (1987) 1.
[35] S.I. Hong, Z. Wang, G.T. Gray III, Mater. Sci. Eng. A 221 (1996) 38.
[36] I. Shiota, M. Suzuki, in: S. Ochiai (Ed.), Mechanical Properties of Metallic Composites, Marcel Dekker, New York, 1994, p. 681.
[37] Jeong, D.K. Hsu, R.E. Shannon, P.K. Liaw, in: P.K. Liaw, O. Buck, S.M. Wolf (Eds.), Nondestructive Evaluation and Materials Properties of advanced Materials, The Minerals, Metals and Materials Society, 1991, p. 37.
[38] W.F. Smith, Metall. Trans. 4 (1973) 2435.
[39] H. Cordier, W. Gruhl, Z. Metallkde 56 (1965) 669.
[40] R.J. Livak, Metall. Trans. 13A (1982) 1324.

[41] L.F. Mondolfo, Aluminum Alloys: Structure and Properties, Butterworths, London, 1976, p. 566.
[42] D.A. Rigney, W.A. Glaeser, Wear 46 (1978) 241.
[43] D.A. Rigney, L.H. Chen, M.G.S. Naylor, A.R. Rosenfield, Wear 100 (1984) 195.
[44] P. Heilmann, W.A.T. Clark, D.A. Rigney, Acta Metall. 31 (1983) 1293.
[45] J.P. Hirth, D.A. Rigney, in: F.R.N. Nabarro (Ed.), Dislocations in Solids, vol. 6, North-Holland, Amsterdam, 1983, p. 1.
[46] T.F.J. Quinn, Friction, Lubrication and Wear Technology, ASM Handbook, vol. 18, ASM International Handbook Committee, 1995, p. 281.
[47] D.H. Kim, D.Y. Maeng, J.H. Lee, J.S. Song, S.I. Hong, C.W. Won, J. Korean Inst. Metall. Mater. 36 (1998) 883.
[48] B.D. Agarwal, L.J. Broutman, Analysis and Performance of Fiber Composites, Wiley, New York, 1990, p. 59.
[49] C. Laird, in: F.R.N. Nabarro (Ed.), Dislocations in Solids, vol. 6, North-Holland, Amsterdam, 1983, p. 60.
[50] S.I. Hong, C. Laird, Metall. Trans. 22A (1991) 415.
[51] S.I. Hong, C. Laird, Acta Metall. 38 (1990) 11.